
Article

Direct Comparison of Chol-siRNA Polyplexes and Chol-DsiRNA Polyplexes Targeting STAT3 in a Syngeneic Murine Model of TNBC

Zhen Ye ², Mai Mohamed Abdelmoaty ^{2,3}, Stephen M. Curran ², Shetty Ravi Dyavar ^{4,#}, Devendra Kumar ², Yazen Alnouti ², Don W. Coulter ⁵, Anthony T. Podany ⁴, Rakesh K. Singh ^{1,6}, Joseph A. Vetro ^{1,2,*}

¹ Center for Drug Delivery and Nanomedicine and ²Department of Pharmaceutical Sciences, College of Pharmacy, University of Nebraska Medical Center, Omaha, Nebraska 68198, USA

³ Therapeutic Chemistry Department, Pharmaceutical and Drug Industries Research Division, National Research Centre, Giza, Egypt

⁴ Department of Pharmacy Practice, College of Pharmacy, University of Nebraska Medical Center, Omaha, Nebraska 68198, USA

⁵ Department of Pediatrics, Division of Pediatric Hematology/Oncology, Department of Radiation Oncology, J. Bruce Henriksen Cancer Research Laboratories, University of Nebraska Medical Center, Omaha, NE 68198-2168, USA

⁶ Department of Pathology and Microbiology, University of Nebraska Medical Center, Omaha, NE 68198-5900, USA

Current address: Adicet Bio, Inc., 200 Constitution Dr, Menlo Park, CA, 94025

* Correspondence: jvetro@unmc.edu; Tel.: 402-559-9359

Abstract: RNA interference (RNAi) molecules have tremendous potential for cancer therapy but are limited by insufficient potency after i.v. administration. We previously found that polymer complexes (polyplexes) formed between 3'-cholesterol-modified siRNA (Chol-siRNA) or DsiRNA (Chol-DsiRNA) and the cationic diblock copolymer PLL[30]-PEG[5K] greatly increase RNAi potency against stably expressed LUC mRNA in primary syngeneic murine breast tumors after daily i.v. dosing. Chol-DsiRNA Polyplexes, however, maintain LUC mRNA suppression ~48 h longer after the final dose than Chol-siRNA Polyplexes, suggesting they are a better candidate formulation. Here, we directly compared the activities of Chol-siRNA and Chol-DsiRNA Polyplexes in primary murine 4T1 breast tumors against STAT3, a therapeutically relevant target gene overexpressed in many solid tumors including breast cancer. We found that Chol-siSTAT3 Polyplexes suppressed STAT3 mRNA in 4T1 tumors with similar potency (half-maximal ED₅₀ 0.3 mg/kg) and kinetics over 96 hours as Chol-DsiSTAT3 Polyplexes but with slightly lower activity against total Stat3 protein (29% vs. 42% suppression) and tumor growth (11.5% vs. 8.6% rate-based T/C ratio) after repeated i.v. administration of tumor-saturating doses every other day. Thus, both Chol-siRNA Polyplexes and Chol-DsiRNA Polyplexes may be suitable clinical candidates for RNAi therapy of breast cancer and other solid tumors.

Keywords: RNAi, drug delivery, siRNA delivery, DsiRNA delivery, RNAi delivery, Chol-DsiRNA polymer micelles, Chol-siRNA polymer micelles

1. Introduction

RNA interference (RNAi) is a natural, intracellular process that selectively decreases the expression of a specific protein at the mRNA level through complementary base-pair binding of gene-specific dsRNA molecules including microRNA (miRNA), small, interfering RNA (siRNA), or dicer-substrate siRNA (DsiRNA) ("RNAi molecules") [1,2]. Several proteins have been identified in tumor or tumor-associated cells where suppression may produce a therapeutic effect and/or increase the efficacy of other cancer treatments [2,3]. Thus, RNAi molecules have tremendous potential for improving cancer therapy.

Most cancer therapies require i.v. administration to reach diffuse or inaccessible tumors [4]. The potencies of RNAi molecules after i.v. administration, however, are extremely low or undetectable [1]. Several types of nanoscale dosage forms have been developed to increase the potency of RNAi molecules after i.v. administration using a wide range of modified RNAi molecules and/or materials [5-7]. We previously found that electrostatically self-assembled polymer complexes (polyplexes) composed of siRNA or DsiRNA modified with 3'-cholesterol on the sense strand (Chol-siRNA / Chol-DsiRNA) and a block copolymer of 30 poly-L-lysine residues and 5 kDa polyethylene glycol (PLL[30]-PEG[5K]) (**Fig.1**) greatly increase RNAi potency against stably expressed LUC mRNA in primary 4T1-Luc breast tumors after daily i.v. administration [2.5 mg Chol-RNAi/kg] over three days without affecting body weight [4,8]. Chol-DsiRNA Polyplexes, however, maintain LUC mRNA suppression ~48 hours longer after the final dose than Chol-siRNA Polyplexes [4,8], have higher loading (50 wt% vs. 25 wt%), provide greater protection against RNase degradation in 90% murine serum, and are well tolerated by healthy female BALB/c mice to at least 50 mg Chol-DsiRNA/kg [2]. This suggests that Chol-DsiRNA Polyplexes are a more promising formulation candidate than Chol-siRNA Polyplexes for RNAi therapy of breast and possibly other solid tumors.

In contrast to suppression of stably expressed LUC mRNA in 4T1-Luc tumors, we recently found that Chol-DsiRNA Polyplexes targeting STAT3, a more widely expressed and therapeutically relevant mRNA, maintain suppression of STAT3 mRNA in primary 4T1 breast tumors less than 24 h after a single lower dose of Chol-DsiSTAT3 [0.5 mg/kg] [2]. Thus, it remains unclear whether or under what conditions Chol-DsiRNA Polyplexes also maintain the suppression of therapeutically relevant mRNA in primary 4T1 tumors for a longer duration than Chol-siRNA Polyplexes. In this study, we address possible differences in Polyplex activities against therapeutically relevant mRNA in solid tumors by directly comparing the activities of Chol-siRNA Polyplexes and Chol-DsiRNA Polyplexes targeting STAT3 in primary 4T1 breast tumors after i.v. administration.

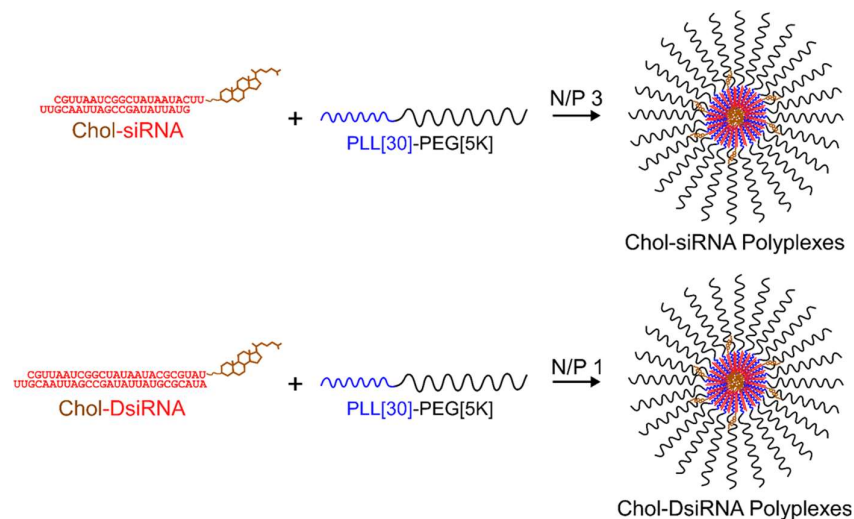


Figure 1. Idealized electrostatic self-assembly of Chol-siRNA and Chol-DsiRNA Polyplexes formed with PLL[30]-PEG[5K]. A solution of negatively-charged siRNA or DsiRNA (red) modified with 3'-cholesterol on the sense strand (brown) is added to a solution of positively-charged diblock copolymers composed of 30 poly-L-lysine residue blocks (blue) and 5 kDa polyethylene glycol blocks (black) (PLL[30]-PEG[5K]) at the indicated N/P charge molar ratio of mole(s) positively-charged primary amines (N) / mole negatively charged phosphates (P). The negatively-charged phosphate backbones of Chol-siRNA or Chol-DsiRNA then electrostatically bind and neutralize the positively-charged PLL[30] blocks. This converts PLL[30]-PEG[5K] unimers into amphiphilic diblock copolymers that spontaneously self-assemble into Chol-siRNA or Chol-DsiRNA polymer complexes (Polyplexes) that are further stabilized by hydrophobic interactions between 3'-cholesterol groups.

2. Results

2.1. Activities of 5'-overlapping siSTAT3 and DsiSTAT3 sequences in murine syngeneic 4T1 breast cancer epithelial cells

Differences in the activities of Chol-siRNA and Chol-DsiRNA Polyplexes after i.v. administration may be due, in part, to differences in the activities of the respective siRNA and DsiRNA sequences in the target cell. We previously found that electroporation with equimolar concentrations of a siLUC sequence or 5'-overlapping DsiLUC sequence (i.e., a 3'-extension of the siLUC sequence) suppresses stably expressed LUC mRNA in 4T1-Luc cells to the same extent and duration over 72 hours [8]. As such, we expected that 5'-overlapping siSTAT3 and DsiSTAT3 sequences would have similar activities against murine STAT3 mRNA in 4T1 cells.

To determine if the activities of 5'-overlapping siSTAT3 and DsiSTAT3 sequences against STAT3 mRNA are similar in murine syngeneic breast cancer epithelial cells, we electroporated 4T1 cells with equimolar concentrations of siSTAT3, DsiSTAT3 (3'-extension of the siSTAT3 sequence that suppresses 81% of murine STAT3 mRNA in 4T1 cells 48 h after electroporation [2]), inactive siCTRL, or inactive DsiCTRL and compared normalized murine STAT3 mRNA copy numbers vs. electroporated 4T1 cells at 24, 48, and 72 h after treatment by RT-ddPCR (Fig.2A). Electroporation with siSTAT3 (Fig.2A, grey circles, dashed line) decreased STAT3 mRNA copy numbers to the same extent as electroporation with DsiSTAT3 (Fig.2A, grey squares, solid line) at 24, 48, and 72 h. In contrast, electroporation with siCTRL (Fig.2A, white circle) or DsiCTRL (Fig.2A, white square) had no effect after 24 h, indicating that suppression of murine STAT3 mRNA is due to the respective siSTAT3 and DsiSTAT3 sequences. Thus, the activities of the current 5'-overlapping siSTAT3 and DsiSTAT3 sequences are similar in syngeneic breast cancer epithelial cells over 72 h.

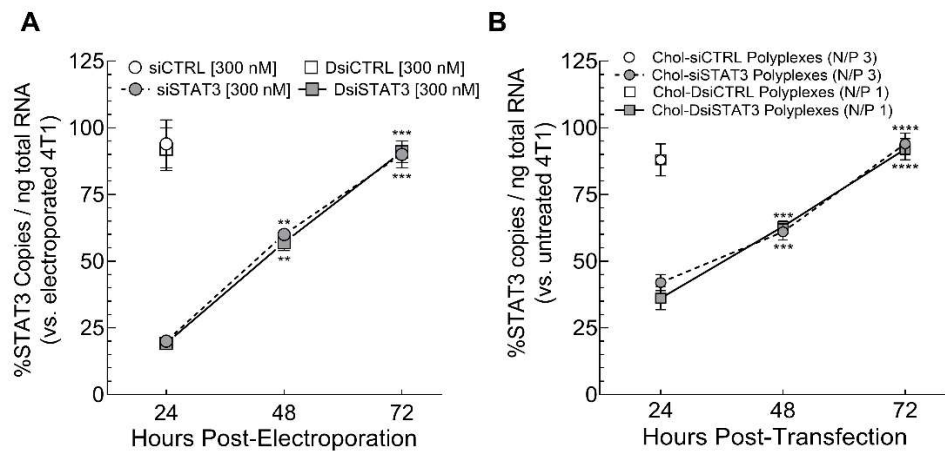


Figure 2. Activities of 5'-overlapping siSTAT3 and DsiSTAT3 sequences and corresponding Chol-siSTAT3 Polyplexes and Chol-DsiSTAT3 Polyplexes in murine 4T1 breast cancer epithelial cells over 72 hours. Murine 4T1 cells were (A) electroporated alone or in the presence of inactive siCTRL (white circle), inactive DsiCTRL (white square), siSTAT3 (grey circles, dashed line), or 5'-overlapping DsiSTAT3 (grey squares, solid line) [300 nM] then incubated at 37°C or (B) incubated 4 h with serum-free media alone or containing inactive Chol-siCTRL (white circle), inactive Chol-DsiCTRL (white square), Chol-siSTAT3 (grey circles, dashed line), or 5'-overlapping Chol-DsiSTAT3 (grey squares, solid line) [200 nM] complexed with PLL[30]-PEG[5K] at the indicated N/P ratio before adding media containing 20% FBS at 1/1 (v/v) and incubating at 37°C. Average murine STAT3 mRNA copy numbers per ng total RNA \pm propagated SD (n=2 (A) or 3 (B) independent treatments) were determined at the indicated time points by RT-ddPCR, normalized to electroporation-only 4T1 cells (A) or untreated 4T1 cells (B) at the same time point, respectively. Averages were then compared at each time point by unpaired two-tailed t-test (no significant differences observed) or vs. the 24 h time point by ordinary one-way ANOVA with Dunnett's post-test where **P

< 0.01, *** P < 0.001, **** P < 0.0001 (siSTAT3 above symbols / DsiSTAT3 below symbols). Results are representative of at least two independent experiments. Data for DsiCTRL, DsiSTAT3, Chol-DsiCTRL, and Chol-DsiSTAT3 taken from [2].

2.2 Hydrodynamic diameters and surface charges of Chol-siRNA and Chol-DsiRNA Polyplexes

Polyplex diameter and surface charge are two physicochemical properties that can potentially affect the activity of polyplexes after i.v. administration (REF). To determine if there are differences in the hydrodynamic diameters and surface charges of Chol-siRNA and Chol-DsiRNA Polyplexes, we compared average hydrodynamic diameters and zeta potentials of Chol-siCTRL and Chol-DsiCTRL Polyplexes in the i.v. administration buffer (0.1 M HEPES, pH 7.4) by nanoparticle tracking analysis and DLS, respectively (**Table 1**). Chol-siCTRL Polyplexes had a slightly smaller hydrodynamic diameter than Chol-DsiCTRL Polyplexes [25 ± 2 (SD) vs. 33 ± 2 nm, $P = 0.0080$, $n = 3$ independent analyses] but a similar zeta potential [8 ± 2 (SD) vs. 5.2 ± 0.7 mV, $P = 0.0840$, $n = 3$ independent analyses] (**Table 1**). Thus, Chol-siRNA and Chol-DsiRNA Polyplexes have slightly different hydrodynamic diameters but similar surface charges.

Table 1. Representative characteristics of Chol-siCTRL Polyplexes and Chol-DsiCTRL Polyplexes.

Polyplex	Endotoxin ¹	Drug Loading	Diameter ²	Zeta Potential ³
	EU/mg (\pm SD)	Wt% Chol-RNAi	nm (\pm SD)	mV (\pm SD)
Chol-siCTRL Polyplexes (N/P 3)	0.122 (0.003)	25	25 (2)	8 (2)
Chol-DsiCTRL Polyplexes (N/P 1)	0.023 (0.002)	50	33 (2)	5.2 (0.7)

¹Determined by endochrome-K™ kit. ²Determined by nanoparticle tracking analysis in 0.1 M HEPES, pH 7.4 and calculated from an average nonlinear fit of the lognormal distribution of Polyplex diameters ($n=3$ independent analyses) (**Figure S2**). ³Determined by DLS in 0.1 M HEPES, pH 7.4 as an average of three independent analyses. Data for Chol-DsiCTRL Polyplexes taken from [2].

2.3 Activities of Chol-siSTAT3 Polyplexes and Chol-DsiSTAT3 Polyplexes in murine syngeneic 4T1 breast cancer epithelial cells

Differences in the activities of Chol-siRNA and Chol-DsiRNA Polyplexes in primary tumors after i.v. administration may be due, in part, to differences in the activities of the respective Chol-siRNA and Chol-DsiRNA Polyplexes in the target cell. To determine if there are differences in the activities of Chol-siRNA and Chol-DsiRNA Polyplexes against STAT3 mRNA in syngeneic murine breast cancer epithelial cells, we transfected 4T1 cells with equimolar concentrations of corresponding Chol-DsiCTRL, Chol-siCTRL, Chol-siSTAT3, or Chol-DsiSTAT3 sequences (**Fig.2A**) complexed with PLL[30]-PEG[5K] at the indicated N/P ratio and compared normalized murine STAT3 mRNA copy numbers to untreated 4T1 cells 24, 48, and 72 h after treatment by RT-ddPCR (**Fig.2B**). Transfection with Chol-siSTAT3 Polyplexes (**Fig.2B**, grey circles, dashed line) decreased STAT3 mRNA copy numbers below untreated 4T1 cells to the same extent as Chol-DsiSTAT3 Polyplexes (**Fig.2B**, grey squares, solid line) at each time point. In contrast, transfection with Chol-siCTRL Polyplexes (**Fig.2B**, white circle) or Chol-DsiCTRL Polyplexes (**Fig.2B**, white square) decreased STAT3 mRNA copy numbers by 12% at 24 h, indicating that STAT3 mRNA suppression by Chol-siSTAT3 or Chol-DsiSTAT3 Polyplexes is primarily due to the activities of complexed Chol-siSTAT3 or Chol-DsiSTAT3, respectively. Thus, the activities of the current Chol-siSTAT3 and Chol-DsiSTAT3 Polyplexes are similar in syngeneic murine breast cancer epithelial cells over 72 h at the current N/P ratios.

2.4 Potencies of Chol-siSTAT3 and Chol-DsiSTAT3 Polyplexes in primary murine syngeneic 4T1 breast tumors after i.v. administration

To determine potential differences between the potencies and efficacies of Chol-siRNA and Chol-DsiRNA Polyplexes against STAT3 mRNA in primary murine syngeneic

breast tumors after i.v. administration, we intravenously administered increasing equimolar doses of Chol-siSTAT3 or Chol-DsiSTAT3 or a single maximum equimolar dose of inactive Chol-siCTRL or inactive Chol-DsiCTRL complexed with PLL[30]-PEG[5K] at the indicated N/P ratio and compared normalized murine STAT3 mRNA copy numbers in early-stage primary 4T1 breast tumors to vehicle alone by RT-ddPCR (Fig.3A). We chose a 48-hour timepoint given that Chol-DsiSTAT3 Polyplexes maximally suppress STAT3 mRNA in primary murine 4T1 breast tumors 48 hours after i.v. administration [2].

Chol-siSTAT3 Polyplexes (Fig.3A, grey circles) suppressed STAT3 mRNA copy numbers in primary 4T1 breast tumors to a similar extent as Chol-DsiSTAT3 Polyplexes (Fig.3A, grey squares) at the highest equimolar dose [47 ± 5 (SD) vs. $46 \pm 3\%$] with a similar half-maximal ED₅₀ [0.2 Chol-siSTAT3 ± 0.1 (SD) vs. 0.3 Chol-DsiSTAT3 ± 0.1 mg/kg] (Fig.3A, dashed line vs. solid line). In contrast, inactive Chol-siCTRL Polyplexes (Fig.3A, white circle) or inactive Chol-DsiCTRL Polyplexes (Fig.3A, white square) had no effect on STAT3 mRNA levels at the highest equimolar doses of Chol-siSTAT3 or Chol-DsiSTAT3, indicating that STAT3 mRNA suppression by Chol-siSTAT3 and Chol-DsiSTAT3 Polyplexes is due to the activities of complexed Chol-siSTAT3 or Chol-DsiSTAT3, respectively. Thus, Chol-siRNA and Chol-DsiRNA Polyplexes have similar potencies and efficacies against STAT3 mRNA in primary murine syngeneic breast tumors after i.v. administration at the current N/P ratios.

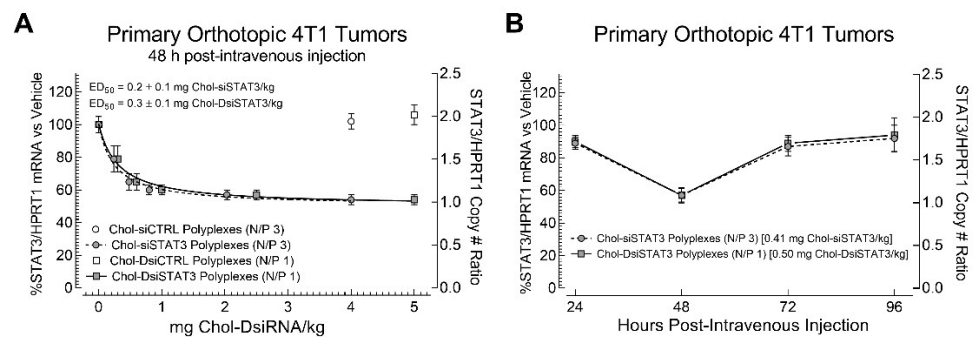


Figure 3. Dose response and kinetics of STAT3 mRNA suppression in primary syngeneic murine breast tumors by Chol-siSTAT3 Polyplexes and Chol-DsiSTAT3 Polyplexes after i.v. administration. (A) Vehicle alone (HEPES/0.15 M NaCl; 0.1 mL) or vehicle containing the indicated dose of Chol-siSTAT3 (grey circles, dashed line), Chol-DsiSTAT3 (grey squares, solid line), inactive Chol-siCTRL (white circle), or inactive Chol-DsiCTRL (white square) complexed with PLL[30]-PEG[5K] at the indicated N/P ratio was injected into the tail veins of female BALB/c mice bearing a single subcutaneous 4T1 breast tumor (~30 to 50 mm³). After 48 hours, average ratios of murine STAT3 to murine HPRT1 mRNA copy numbers in primary 4T1 breast tumors \pm propagated SD (n=5 mice) were determined by RT-ddPCR and half-maximal ED₅₀ values were calculated for each polyplex from nonlinear fits of their respective dose-response curve. (B) Vehicle alone (HEPES/0.15 M NaCl; 0.1 mL) or vehicle containing an equimolar dose of Chol-siSTAT3 (grey circles, dashed line) or Chol-DsiSTAT3 (grey squares, solid line) complexed with PLL[30]-PEG[5K] at the indicated N/P ratio was injected into the tail veins of female BALB/c mice bearing a single subcutaneous 4T1 breast tumor (~30 to 50 mm³). At the indicated time points after injection, average ratios of murine STAT3 to murine HPRT1 mRNA copy numbers in primary 4T1 breast tumors \pm propagated SD (n=5 mice) were determined by RT-ddPCR then compared at the same time point by Two-Tailed Mann-Whitney test. Data for Vehicle, Chol-DsiCTRL Polyplexes, and Chol-DsiSTAT3 Polyplexes taken from [2]. Results are representative of at least two independent experiments.

2.5 Kinetics of Chol-siSTAT3 and Chol-DsiSTAT3 Polyplex activities in primary murine syngeneic breast tumors after i.v. administration

To determine if there are differences between the kinetics of STAT3 mRNA suppression in primary murine syngeneic breast tumors by Chol-siSTAT3 and Chol-DsiSTAT3 Polyplexes after i.v. administration, we intravenously administered a single equimolar

dose of Chol-siSTAT3 or Chol-DsiSTAT3 complexed with PLL[30]-PEG[5K] at the indicated N/P ratio and compared normalized STAT3 mRNA copy numbers in early-stage primary murine 4T1 breast tumors to vehicle alone every 24 hours over 96 hours by RT-ddPCR (**Fig.3B**). We chose an equimolar dose of Chol-siSTAT3 [0.41 mg/kg] and Chol-DsiSTAT3 [0.5 mg/kg] that does not maximally suppress STAT3 mRNA in primary 4T1 breast tumors (**Fig.3A**) to eliminate possible effects of tumor dose saturation on the kinetics of mRNA suppression in the primary tumor. Chol-siSTAT3 Polyplexes (**Fig.3B**, grey circles, dashed line) suppressed STAT3 mRNA copy numbers in primary 4T1 breast tumors to the same extent as Chol-DsiSTAT3 Polyplexes (**Fig.3B**, grey squares, solid line) at 24 h [11 ± 4 (SD) vs. $10 \pm 4\%$], 48 h [43 ± 4 (SD) vs. $43 \pm 5\%$], 72 h [13 ± 6 (SD) vs. $11 \pm 5\%$], and 96 h [8 ± 8 (SD) vs. $6 \pm 10\%$]. Thus, Chol-siSTAT3 and Chol-DsiSTAT3 Polyplexes suppress STAT3 mRNA in primary murine syngeneic breast tumors with similar kinetics after i.v. administration at the current N/P ratios.

2.6 Activities of Chol-siSTAT3 and Chol-DsiSTAT3 Polyplexes against the growth of primary murine syngeneic breast tumors after i.v. administration

STAT3 is critical for the growth of murine 4T1 breast tumors [9-11]. Thus, to determine if there are differences in the therapeutic activities of Chol-siSTAT3 and Chol-DsiSTAT3 Polyplexes against primary murine syngeneic breast tumors after i.v. administration, we intravenously administered an equimolar dose of Chol-siSTAT3, Chol-DsiSTAT3, inactive Chol-siCTRL, or inactive Chol-DsiCTRL complexed with PLL[30]-PEG[5K] at the indicated N/P ratio every other day to mice bearing early-stage 4T1 breast tumors and compared tumor volumes to vehicle alone over 8 days by 3D surface scanning (**Fig.4A**, **Fig.S2**). We chose the lowest equimolar dose of Chol-siSTAT3 [2 mg/kg] and Chol-DsiSTAT3 [2.5 mg/kg] that provided maximum suppression of STAT3 mRNA levels in primary 4T1 breast tumors (**Fig.3A**) to minimize possible effects of dose saturation in the primary tumor.

Chol-siSTAT3 Polyplexes (**Fig.4A**, grey circles, dashed line) inhibited the growth of primary 4T1 tumors at a slightly higher rate-based T/C ratio [12] than Chol-DsiSTAT3 Polyplexes (**Fig.4A**, grey squares, solid line) vs. vehicle alone (**Fig.4A**, white triangles) [11.5% vs. 8.6%] where T/C ratios $\leq 10\%$ indicate high anti-tumor activity at non-toxic doses [12]. In contrast, Chol-siCTRL Polyplexes (**Fig.S2**, white circles) or Chol-DsiCTRL Polyplexes (**Fig.S2**, white squares) did not affect the growth of primary murine 4T1 breast tumors vs. vehicle alone (**Fig.S2**, white triangles), indicating that the inhibition of 4T1 tumor growth was due to the activities of complexed Chol-siSTAT3 or Chol-DsiSTAT3, respectively. Consistent with slightly lower therapeutic activity against primary 4T1 breast tumor growth (**Fig.4A**), Chol-siSTAT3 Polyplexes (**Fig.4C**, grey bar) suppressed 13% less total Stat3 protein in primary 4T1 tumors than Chol-DsiSTAT3 Polyplexes (**Fig.4C**, black bar) vs. vehicle alone 48 h after the final i.v. dose (Day 8) [29 ± 2 (SD) vs. $42 \pm 2\%$ suppression]. Furthermore, average body weights of mice from all treatment groups gradually increased over the course of the study (not shown), indicating that (i.) Chol-siSTAT3 and Chol-DsiSTAT3 Polyplexes are not toxic under the current dosage regimen and (ii.) tumor growth inhibition is due to the activity of complexed Chol-siSTAT3 or Chol-DsiSTAT3 and not abnormal weight loss. Thus, Chol-siSTAT3 Polyplexes have slightly lower therapeutic activity against primary murine syngeneic breast tumors than Chol-DsiSTAT3 Polyplexes with the current dosage regimen and N/P ratios.

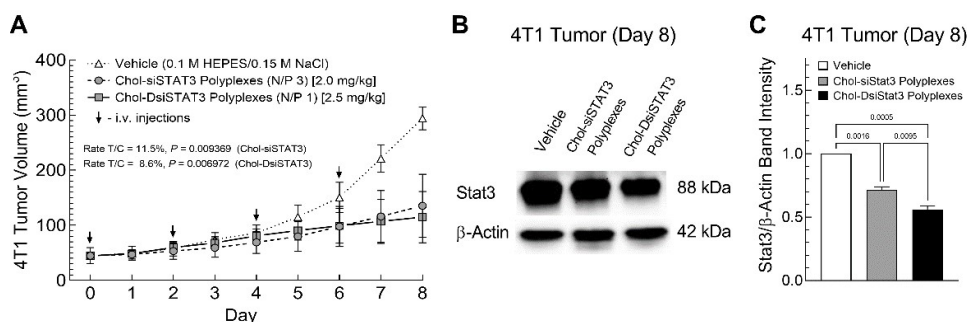


Figure 4. Effect of Chol-siSTAT3 Polyplexes and Chol-DsiSTAT3 Polyplexes on primary syngeneic murine breast tumor growth and STAT3 protein expression after multiple i.v. treatments. (A) Vehicle alone (white triangles) or vehicle containing equimolar doses of inactive Chol-siCTRL (Fig.S2, white circles), inactive Chol-DsiCTRL (Fig.S2, white squares), Chol-siSTAT3 (grey circles), or Chol-DsiSTAT3 (grey squares) complexed with PLL[30]-PEG[5K] at the indicated N/P ratio was injected into the tail veins of 4 to 6 week old female BALB/c mice (black arrows) bearing a single subcutaneous 4T1 breast tumor (~30 to 50 mm³). Average daily tumor volumes \pm SD (n=5 mice) were then determined by 3D surface scanning, compared at each time point by Multiple Mann-Whitney tests (polyplexes), and a rate-based T/C ratio with associated *P* value was calculated for each polyplex (B) On Day 8 (48 h after final i.v. injection), steady-state levels of murine STAT3 and murine β -Actin protein in primary 4T1 tumors were determined by Western Blot then (C) average ratios of Stat3/ β -Actin protein band intensities \pm SD (n=2 measurements) were determined by imaging densitometry and compared by ordinary one-way ANOVA. Protein bands from images of the same Western blot were used to generate (B). Data for vehicle, Chol-DsiCTRL, and Chol-DsiSTAT3 taken from [2]. Results are representative of at least two independent experiments.

2.7 Pharmacokinetics of Chol-DsiSTAT3 and Chol-DsiSTAT3 Polyplexes in healthy female BALB/c mice after i.v. administration

To next determine if there are differences between the pharmacokinetics of complexed Chol-siRNA and Chol-DsiRNA, we intravenously administered equimolar doses of Chol-siSTAT3 or Chol-DsiSTAT3 alone or complexed with PLL[30]-PEG[5K] at the indicated N/P ratio into young healthy female BALB/c mice. Given that total RNA in plasma from untreated mice is relatively constant (not shown), we then indirectly determined plasma concentrations of Chol-siSTAT3 or Chol-DsiSTAT3 over time as an increase in total RNA extracted from the plasma of treated vs. untreated mice (Fig.5) for pharmacokinetic analysis (Table 2).

The high variability of plasma concentrations and limited number of time points (Fig.5A&B) prevented complete and accurate compartmental analysis of the PK profiles. Despite the limited analysis, uncomplexed Chol-siSTAT3 and Chol-DsiSTAT3 had a statistically similar AUC [2.3 ± 0.9 (SD) vs. 3 ± 1 h* μ g/mL, *P* = 0.2782] and mean residence time [0.07 ± 0.03 (SD) vs. 0.8 ± 0.9 h, *P* = 0.1074] (Table 2). Although Chol-siSTAT3 Polyplexes increased the AUC [19 ± 2 (propagated SD) vs. 13 \pm 2-fold increase in AUC, *P* < 0.0021] and mean residence time [7.1 ± 0.5 (propagated SD) vs. 1 \pm 1-fold increase in MRT, *P* < 0.0001] vs. uncomplexed Chol-siSTAT3 to a greater extent than Chol-DsiSTAT3 Polyplexes vs. uncomplexed Chol-DsiSTAT3 (Table 2), complexed Chol-siSTAT3 and Chol-DsiSTAT3 had a similar AUC [44 ± 2 (SD) vs. 39 ± 13 h* μ g/mL, *P* = 0.4200] and mean residence time [0.5 ± 0.5 (SD) vs. 0.9 ± 0.4 h, *P* = 0.2000] (Table 2). Thus, Chol-siSTAT3 Polyplexes and Chol-DsiSTAT3 Polyplexes increase plasma exposure and mean residence time of complexed Chol-siSTAT3 and Chol-DsiSTAT3 to similar levels in young healthy female BALB/c mice at the current N/P ratios.

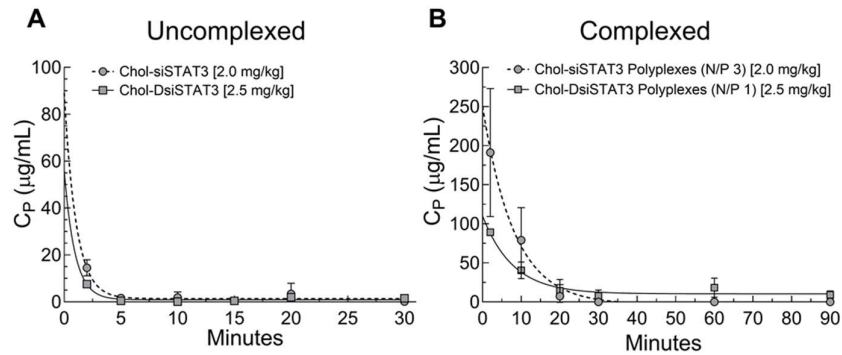


Figure 5. Pharmacokinetics of complexed Chol-siSTAT3 and Chol-DsiSTAT3 in healthy young female BALB/c mice after i.v. administration. An equimolar dose of Chol-siSTAT3 [2.0 mg/kg] (black circles) or Chol-DsiSTAT3 [2.5 mg/kg] (grey squares) (A) alone or (B) complexed with PLL[30]-PEG[5K] at the indicated N/P ratio was injected into the tail veins of healthy female BALB/c mice (4 to 6 weeks old) and average plasma concentrations of Chol-siSTAT3 or Chol-DsiSTAT3 \pm SD ($n = 5$ mice), respectively, were determined indirectly at each time point as differences in total extracted RNA from the plasma of treated vs. untreated mice by fluorescence assay. Error bars are present in (A) but sometimes indistinguishable at the current scale. Data for Chol-DisRNA and Chol-DsiRNA Polyplexes taken from [2].

Table 2. Pharmacokinetic parameters of Chol-siSTAT3, Chol-DsiSTAT3, Chol-siSTAT3 Polyplexes, and Chol-DsiSTAT3 Polyplexes in healthy young female BALB/c mice after i.v. administration.

PK Parameter	Chol-siSTAT3 (\pm SD)	Chol-siSTAT3 Polyplexes (\pm SD)	Chol-DsiSTAT3 (\pm SD)	Chol-DsiSTAT3 Polyplexes (\pm SD)
C_0 (μ g/mL)	89 (65)	250 (123)	56 (64)	110 (7)
$AUC_{0-\infty}$ ($h \cdot \mu$ g/mL)	2.3 (0.9)	44 (2)	3 (1)	39 (13)
$MRT_{0-\infty}$ (h)	0.07 (0.03)	0.5 (0.5)	0.8 (0.9)	0.9 (0.4)

Average plasma concentration at time point = 0 (C_0) and mean residence time ($MRT_{0-\infty}$) in healthy female BALB/c mice (4 to 6 weeks old) were determined by non-compartmental analysis (Phoenix WinNonlin) and average area under the curve ($AUC_{0-\infty}$) of Chol-DsiSTAT3 ($n = 5$ mice) was determined by the linear log trapezoidal rule of the respective PK profiles (Fig.5). Data for Chol-DisRNA and Chol-DsiRNA Polyplexes taken from [2].

2.8 Distribution of Chol-DsiSTAT3 and Chol-DsiSTAT3 Polyplexes in 4T1 breast tumor-bearing female BALB/c mice

To next determine if there are differences in the distributions of complexed Chol-siSTAT3 and Chol-DsiSTAT3 after i.v. administration, we intravenously administered an equimolar dose of Chol-siSTAT3 or Chol-DsiSTAT3 alone or complexed with PLL[30]-PEG[5K] at the indicated N/P ratio into young 4T1 breast tumor-bearing female BALB/c mice and compared the distributions of Chol-siSTAT3 or Chol-DsiSTAT3 in perfused organs and 4T1 breast tumors fifteen minutes post-injection by RT-ddPCR of the anti-sense strand (Fig.6). We chose a fifteen-minute time point to minimize RNase degradation of distributed Chol-siRNA and Chol-DsiRNA molecules [7].

Uncomplexed Chol-siSTAT3 had a similar distribution as uncomplexed Chol-DsiSTAT3 in the tumor [0.46 ± 0.1 (SD) vs. 0.6 ± 0.2 ng/mg tissue, $P = 0.0588$], brain [0.013 ± 0.001 (SD) vs. 0.03 ± 0.07 ng/mg tissue, $P = 0.6890$], kidneys [1.0 ± 0.2 (SD) vs. 1.0 ± 0.4 ng/mg tissue, $P = 0.8206$], lungs [0.43 ± 0.05 (SD) vs. 0.41 ± 0.05 ng/mg tissue, $P = 0.4680$], and liver [0.85 ± 0.09 (SD) vs. 0.9 ± 0.2 ng/mg, $P = 0.4692$] but a slightly lower distribution than uncomplexed Chol-DsiSTAT3 in the heart [0.020 ± 0.003 (SD) vs. 0.029 ± 0.005 ng/mg, $P = 0.0078$] and spleen [1.4 ± 0.2 (SD) vs. 2.3 ± 0.4 ng/mg, $P = 0.0067$] (Fig.6). Chol-siRNA

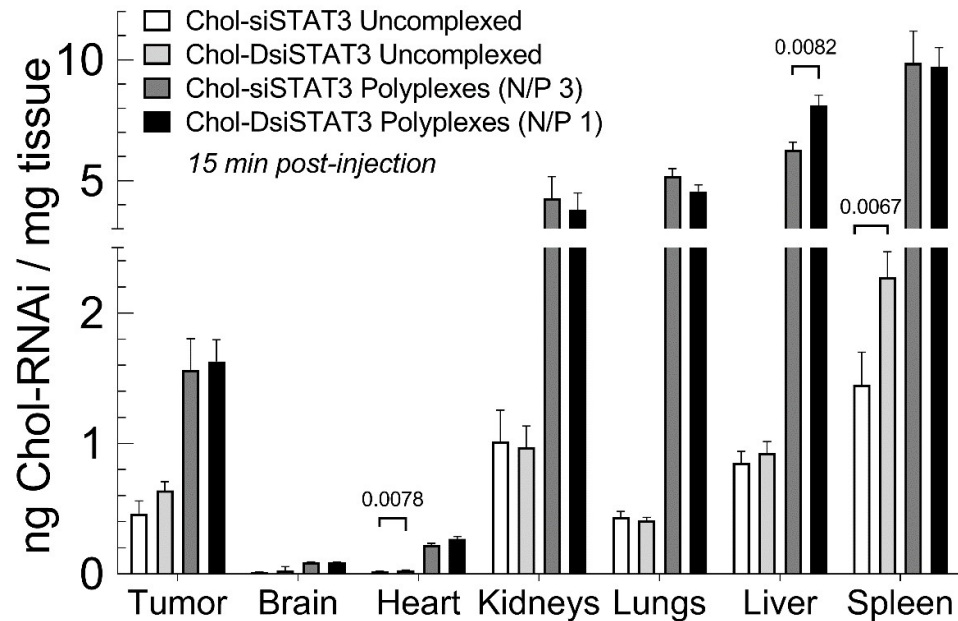


Figure 6. Effect of Chol-siRNA Polyplexes and Chol-DsiRNA Polyplexes on the distribution of Chol-siSTAT3 and Chol-DsiSTAT3 in syngeneic 4T1 breast tumor-bearing mice after i.v. administration. An equimolar dose of Chol-siSTAT3 [2.0 mg/kg] or Chol-DsiSTAT3 [2.5 mg/kg] alone or complexed with PLL[30]-PEG[5K] at the indicated N/P ratio was injected i.v. into female BALB/c mice bearing a single 4T1 breast tumor (~30 to 50 mm³). After 15 minutes, average ng of Chol-DsiSTAT3/mg tissue \pm propagated SD (n=5 mice) was determined by RT-ddPCR of the respective antisense strands and compared (uncomplexed vs. uncomplexed; polyplex vs. polyplex) in each tissue by unpaired two-tailed t-tests. The Y-axis was truncated to facilitate comparison between treatment groups. Data for Chol-DsiSTAT3 and Chol-DsiSTAT3 Polyplexes taken from (REF).

Polyplexes, except for a greater increase in the spleen [7 ± 2 (SD) vs. 4 ± 1 ng/mg tissue increase vs. uncomplexed Chol-RNAi molecule, $P = 0.0171$], increased the distribution of complexed Chol-siSTAT3 vs. uncomplexed Chol-siSTAT3 to a similar extent as Chol-DsiSTAT3 Polyplexes vs. uncomplexed Chol-DsiSTAT3 in the tumor, brain, heart, kidneys, lungs, and liver (Fig.6). Complexed Chol-siSTAT3 also had a similar distribution as complexed Chol-DsiSTAT3 in the tumor [1.6 ± 0.5 (SD) vs. 1.6 ± 0.4 ng/mg tissue, $P = 0.8294$], brain [0.09 ± 0.01 (SD) vs. 0.088 ± 0.007 ng/mg tissue, $P = 0.9557$], heart [0.22 ± 0.03 (SD) vs. 0.27 ± 0.04 ng/mg tissue, $P = 0.0828$], kidneys [4 ± 2 (SD) vs. 4 ± 2 ng/mg tissue, $P = 0.6902$], lungs [5.2 ± 0.7 (SD) vs. 4.6 ± 0.6 ng/mg tissue, $P = 0.1693$], and spleen [10 ± 3 (SD) vs. 10 ± 2 ng/mg tissue, $P = 0.9178$] but a slightly lower distribution in the liver [6.3 ± 0.7 (SD) vs. 8.1 ± 0.9 ng/mg tissue, $P = 0.0082$]. Thus, except for the liver, Chol-siRNA and Chol-DsiRNA Polyplexes increase the distribution of complexed Chol-siSTAT3 and Chol-DsiSTAT3, respectively, to a similar extent in syngeneic breast tumors and other organs in female BALB/c mice after i.v. administration at the current N/P ratios.

3. Discussion

Our study provides evidence that Chol-siRNA Polyplexes suppress an endogenous, therapeutically relevant target gene in early-stage primary syngeneic murine breast tumors with similar potency, efficacy, and kinetics as Chol-DsiRNA Polyplexes but slightly lower therapeutic activity after repeated i.v. administration at the current N/P ratios. We found that Chol-siRNA Polyplexes (N/P 3) and Chol-DsiRNA Polyplexes (N/P 1) suppressed STAT3 mRNA in primary murine 4T1 breast tumors (~30 to 50 mm³) at similar potencies [half-maximal ED₅₀ of 0.2 ± 0.1 mg Chol-siSTAT3/kg vs. 0.3 ± 0.1 mg Chol-DsiSTAT3/kg] (Fig.3A), efficacies [47% Emax] (Fig.3A), and kinetics over 96 h (Fig.3B), whereas Chol-siSTAT3 Polyplexes suppressed lower levels of total Stat3 protein [29% vs.

42%] (**Fig.4C**) and 4T1 tumor growth [rate-based T/C ratio of 11.5% vs. 8.6%] (**Fig.4A**) after repeated i.v. administration every other day.

Our study also provides evidence that Chol-siSTAT3 and Chol-DsiSTAT3 Polyplexes increase plasma exposure of complexed Chol-RNAi molecules to similar levels in young, healthy female BALB/c mice as well as localization to primary syngeneic murine breast tumors after i.v. administration at the current N/P ratios. We found that Chol-siRNA Polyplexes and Chol-DsiRNA Polyplexes (i.) increased the AUC [44 ± 2 (SD) vs. 39 ± 13 h* $\mu\text{g}/\text{mL}$, $P = 0.4200$] and mean residence time [0.5 ± 0.5 (SD) vs. 0.9 ± 0.4 h, $P = 0.2000$] of complexed Chol-siSTAT3 and Chol-DsiSTAT3, respectively, to similar levels in healthy, 4 to 6 week old female BALB/c mice (**Table 2**) and (ii.) increased the distribution of complexed Chol-siSTAT3 and Chol-DsiSTAT3, respectively, to similar levels in primary 4T1 breast tumors 15 minutes after i.v. administration [1.6 ± 0.5 (SD) vs. 1.6 ± 0.4 ng/mg tissue] (**Fig.6**).

A key finding of the present study is that both Chol-siSTAT3 Polyplexes and Chol-DsiSTAT3 Polyplexes maintain the suppression of STAT3 mRNA in primary 4T1 breast tumors less than 24 h after i.v. administration of a single dose of Chol-RNAi (**Fig.3B**). This differs from our previous study where Chol-DsiLUC Polyplexes maintain the suppression of stably expressed LUC mRNA in primary 4T1-Luc tumors ~48 h longer than Chol-siLUC Polyplexes (72 hr vs. 24 h) after daily i.v. administration over 3 days [8].

One possible reason that Chol-DsiLUC Polyplexes suppress mRNA in primary syngeneic murine breast tumors for a longer duration than Chol-DsiSTAT3 Polyplexes and Chol-siSTAT3 Polyplexes after i.v. administration is that the DsiLUC sequence and/or corresponding Chol-DsiLUC Polyplexes suppress LUC mRNA for a longer duration in 4T1-Luc cells within the primary tumors than siLUC and/or corresponding Chol-siLUC Polyplexes. This is unlikely, however, given electroporation with DsiLUC or siLUC sequences and transfection with corresponding Chol-DsiLUC Polyplexes or Chol-siLUC Polyplexes suppress LUC activity in 4T1-Luc cells with similar potency and kinetics over 72 h [8]. A similar trend was also observed with the current siSTAT3 and DsiSTAT3 sequences (**Fig.2A**) and corresponding Chol-siSTAT3 Polyplexes and Chol-DsiSTAT3 Polyplexes in 4T1 cells (**Fig.2B**).

A second possible reason is that increasing the frequency of tumor-saturating doses increases the duration that Chol-DsiRNA Polyplexes suppress mRNA in primary syngeneic murine breast tumors to a greater extent than Chol-siRNA Polyplexes. This remains a possibility given that (i.) Chol-DsiSTAT3 Polyplexes and Chol-siSTAT3 Polyplexes suppress STAT3 mRNA in primary 4T1 tumors for a similar duration after i.v. administration of a single equimolar dose (**Fig.3B**) that is unlikely to saturate the primary 4T1 tumor [0.50 mg Chol-DsiSTAT3/kg and 0.41 mg Chol-siSTAT3/kg] (**Fig.3A**), whereas Chol-DsiSTAT3 Polyplexes suppress slightly higher levels of total Stat3 protein [42% vs.29%] (**Fig.4C**) and subsequent 4T1 tumor growth [rate-based T/C ratio of 8.6 % vs. 11.5%] than Chol-siSTAT3 Polyplexes after repeated i.v. administration every other day over 6 days (**Fig.4A**) at equimolar doses that are likely to saturate primary 4T1 tumors [2.0 mg Chol-siSTAT3/kg and 2.5 Chol-DsiSTAT3 mg/kg] (**Fig.3A**) and (ii.) Chol-DsiLUC Polyplexes suppress Luc activity in primary 4T1-Luc tumors 48 h longer than Chol-siLUC Polyplexes after daily i.v. administration over 3 days [8] at doses that are also likely to saturate primary 4T1 tumors [2.5 mg/kg] (**Fig.3A**).

4. Materials and Methods

4.1 Polymer

Methoxy-poly(ethylene glycol)-*b*-poly(L-lysine hydrochloride) with a 5 kDa polyethylene glycol block (PEG[5K]) and a 30 poly-L-lysine block (PLL[30]) [PLL[30]-PEG[5K]; avg. MW 9900 Da] was obtained from Alamanda Polymers (Huntsville, AL). The number of Lys residues within the PLL[30] block was $\pm 10\%$ (PLL[27] to PLL[33]) and the polydispersity index of the entire polymer was between 1 and 1.1.

4.2 RNAi Molecules

HPLC-purified siRNA and DsiRNA RNAi with indicated (UU) overhangs was obtained from GE Dharmacon: **(1) siCTRL** sense: 5' – CGU UAA UCG CGU AUA AUA C(UU) – 3', antisense: 5' – GUA UUA UAC GCG AUU AAC G(UU) – 3'; **(2) DsiCTRL** sense: 5' – CGU UAA UCG GCU AUA AUA CGC GUA U – 3', antisense: 5' – AUA CGC GUA UUA UAC GCG AUU AAC G(UU) – 3'; **(3) siSTAT3** sense: 5' – GGU CAA AUU UCC UGA GUU G(UU) – 3', antisense: 5' – CAA CUC AGG AAA UUU GAC C(UU) – 3'; **(4) DsiSTAT3** sense: 5' – GGU CAA AUU UCC UGA GUU GAA UUA U – 3', antisense: 5' – AUA AUU CAA CUC AGG AAA UUU GAC C(UU) – 3'; **(5) Chol-siCTRL** siCTRL with 3'-cholesterol conjugated to the sense strand; **(6) Chol-siSTAT3** siSTAT3 with 3'-cholesterol conjugated to the sense strand; **(7) Chol-DsiCTRL** DsiSTAT3 with 3'-cholesterol conjugated to the sense strand; **(8) Chol-DsiSTAT3** DsiSTAT3 with 3'-cholesterol conjugated to the sense strand. For *in vitro* studies, lyophilized RNAi molecules were resuspended in sterile, nuclease-free ddH₂O [100 µM] as directed (GE Dharmacon) and stored in aliquots [10 µL] at -80°C. For *in vivo* studies, lyophilized RNAi molecules were resuspended in the indicated buffer on the day of injection.

4.3 Cell Culture

Murine 4T1 breast cancer epithelial cells (CRL-2539, ATCC) were cultured in Complete RPMI-1640 Media composed of RPMI 1640 / L-glutamine [1.1481 mM] (GE Healthcare Life Sciences) containing heat-inactivated FBS [10% v/v; endotoxin <0.3 EU scale] (Atlanta Biologicals, Atlanta, GA), sodium pyruvate [1 mM] (Gibco), 1X MEM non-essential amino acids (Hyclone), 1X Vitamins (Hyclone), and penicillin G [100 U/mL] / streptomycin sulfate [100 µg/mL] (Gibco). Cells were grown in TPP plates (MIDSCI, St. Louis, MO) at 37°C / 5% CO₂ and passaged using Accutase (Innovative Cell Technologies, San Diego, CA) as directed.

4.4 Electroporation of Murine 4T1 Cells

Murine 4T1 cells [10 × 10⁶ cells/mL] were electroporated (Nucleofector, Lonza AG, Bazel, Switzerland) with the indicated RNAi molecules [300 nM] using Amaxa Cell Line Kit V for Mouse Epithelial Cells (VCA-1003, Lonza) as directed (Setting T-024) and cultured in 6-well plates [1 × 10⁶ cells / well]. Total RNA was isolated (RNeasy Micro kit, Qiagen) and eluted with sterile, nuclease-free deionized H₂O [20 µL], quantitated by A₂₆₀ (NanoDrop 2000™ Spectrophotometer, Thermo Scientific) [3 µL], and stored at -80°C. Average STAT3 mRNA copies / ng total RNA ± SD (n=2 replicates from two independent electroporations) were determined by RT-ddPCR (Section 4.9), normalized to electroporated 4T1 cells alone at the indicated time points, and compared at each time point by unpaired two-tailed t-test or compared vs. the 24 h time point by ordinary one-way ANOVA with Dunnett's post-test (GraphPad Prism 9.2.0).

4.5 Formation of Chol-RNAi Polyplexes

The concentration of a 2X Polymer Complexation Solution at the indicated N/P charge molar ratio of moles positively-charged primary amines (N) from the PLL[30] block of PLL[30]-PEG[5K] to moles negatively-charged phosphates (P) from the phosphate backbone of Chol-siRNA [N/P 3] or Chol-DsiRNA [N/P 1] [8] was calculated based on the concentration of the 2X Chol-RNAi Complexation Solution

$$2X \text{ Polymer Complexation Sol'n } \left(\frac{g}{mL} \right) = \frac{g \text{ RNAi}}{mL} \times \frac{mol \text{ RNAi}}{MW \text{ RNAi}} \times \frac{mol \text{ RNAi P}}{mol \text{ RNAi}} \times \frac{mol \text{ Polymer N}}{mol \text{ RNAi P}} \times \frac{mol \text{ Polymer}}{mol \text{ Polymer N}} \times \frac{MW \text{ Polymer}}{mol \text{ Polymer}}$$

where $g \text{ RNAi}/mL$ = Concentration of 2X Chol-RNAi Complexation Solution (Double desired concentration of Chol-RNAi in the final Chol-RNAi Polyplex solution), $MW \text{ RNAi}$ = MW of Chol-RNAi, $mol \text{ RNAi P} / mol \text{ RNAi}$ = 42 (Chol-siRNA) or 52 (Chol-DsiRNA) moles phosphate per mole Chol-RNAi, $mol \text{ Polymer N} / mole \text{ RNAi P}$ = N/P charge molar ratio, $mol \text{ Polymer} / mol \text{ Polymer N}$ = 1 mole of PLL[30]-PEG[5K] / 30 moles PLL primary amines, $MW \text{ Polymer} / mol \text{ Polymer}$ = MW of PLL[30]-PEG[5K] = 9900 Da.

For transfection studies, a Concentrated Stock Solution of Chol-RNAi Polyplexes at the indicated N/P was prepared by (i.) sterilizing PLL[30]-PEG[5K] in open, sterile 2 mL centrifuge tubes under vacuum for 2 h in a desiccator containing a glass dish of 99% ethanol (ii.) preparing a 2X Chol-RNAi Complexation Solution plus 10 μ L for experimental loss by diluting a thawed frozen stock of Chol-RNAi with sterilized (0.2 μ m filter) HEPES Buffer [0.1 M HEPES in deionized H₂O, pH 7.4] to double the desired concentration of Chol-RNAi in the final Concentrated Stock Solution (iii.) preparing a 2X Polymer Complexation Solution plus 10 μ L for experimental loss by dissolving sterilized PLL[30]-PEG[5K] in HEPES Buffer at 1 mg Polymer/mL, incubating at r.t. for 30 min, and diluting with HEPES Buffer to the calculated 2X concentration (iv.) forming a Concentrated Stock Solution of Chol-RNAi Polyplexes by adding the 2X Chol-RNAi Complexation Solution dropwise to the 2X Polymer Complexation Solution at 1/1 (v/v), mixing the solution by pipette aspiration / dispensation (30 sec), and incubating (RT, 30 min.).

For *in vivo* studies, endotoxin-free solutions/reagents and disposables were used under aseptic conditions. A Concentrated Stock Solution of Chol-RNAi alone or Chol-RNAi Polyplexes at the indicated N/P charge molar ratio was prepared on the day of injection by (i.) determining the total volume of Concentrated Chol-RNAi Stock Solution (Chol-RNAi alone and Chol-RNAi Polyplexes) required for all mice in the study based on injected dose (mg/kg), individual mass of each mouse, and total prepared i.v. injection volume [125 μ L per mouse for dose response / kinetics studies] plus 50 μ L for experimental loss (ii.) preparing a 2X Chol-RNAi Complexation Solution (1/2 total required volume of Concentrated Stock Solution of Chol-RNAi) plus 25 μ L for experimental loss by resuspending lyophilized Chol-RNAi as directed by the manufacturer in sterilized HEPES Buffer to double the desired concentration of Chol-RNAi in the Concentrated Stock Solution (iii.) sterilizing PLL[30]-PEG[5K] and preparing 2X Polymer Complexation Solution (same volume as 2X Chol-RNAi Complexation Solution) as described for transfection studies above (iv.) preparing the required volume of Concentrated Stock Solution of Chol-RNAi Polyplexes as described above and (v.) preparing the required volume of Concentrated Stock Solution of Chol-RNAi alone by diluting the 2X Chol-RNAi Complexation Solution 1/1 (v/v) with sterilized HEPES Buffer. The required i.v. injection volume [100 μ L] of Chol-RNAi alone or Chol-RNAi Polyplexes plus 25 μ L for each mouse was then prepared by combining (i.) volume of Concentrated Chol-RNAi or Chol-RNAi Polyplex Stock Solution adjusted to deliver the required dose of Chol-RNAi based on mouse bodyweight (ii.) volume of sterilized (0.2 μ m filter) HEPES Buffer plus 1.5 M NaCl at 1/10 dilution [0.15 M NaCl final conc.], and (iii.) volume of HEPES Buffer adjusted to final volume.

4.6 Hydrodynamic diameters and zeta potentials of Chol-RNAi Polyplexes

Polyplex hydrodynamic diameters were determined by nanoparticle tracking analysis (NanoSight LM10 and NTA 2.3 analytical software, Malvern Instruments, UK). Chol-siCTRL and Chol-DsiCTRL Polyplexes [0.25 mg Chol-RNAi/mL] were prepared in 0.1 M HEPES [pH 7.4] at the indicated N/P ratio as described for Transfection (Section 4.5) and recorded (Shutter speed: 500, Gain: 680) for video analysis (screen gain: 6; solution temperature: 22°C; viscosity: 0.95 cP [viscosity of water at 22°C]; remaining parameters: auto). The average estimated concentration of Chol-RNAi Polyplexes for each 1 nm bin from three independent analyses was normalized as a percentage of the total average estimated concentration of Chol-RNAi Polyplexes. A plot of accumulated percent of total Chol-RNAi Polyplexes at each diameter (y-axis) vs. ln diameter (x-axis) was then fit against a cumulative Gaussian (percent) model (GraphPad Prism 9.2.0) to determine a best-fit mean and standard deviation from the lognormal curve. Average hydrodynamic diameters \pm propagated SD (n =3 independent analyses) were compared by unpaired two-tailed t-test (Graphpad Prism Version 9.2.0).

Polyplex zeta potentials were determined by dynamic light scattering (DLS). Chol-siCTRL and Chol-DsiCTRL Polyplexes [1 mg polymer/mL] were prepared in 0.1 M HEPES [pH 7.4] at the indicated N/P ratio as described for Transfection (Section 4.5). Average

Polyplex zeta potentials \pm propagated SD (n=3 independent measurements \pm SD) were measured using a ZetaSizer Nano ZS (Malvern Instruments, Malvern, UK) equipped with He-Ne laser ($\lambda = 633$ nm) as the incident beam as previously described [4] and compared by unpaired two-tailed t-test (GraphPad Prism 9.2.0).

4.7 Endotoxin levels

Endotoxin levels of Chol-RNAi Polyplexes [0.05 mg Chol-RNAi/mL] were quantitated as directed using an Endochrome-K Limulus Amebocyte Lysate Kit (Charles River Labs) with endotoxin-free reagents and disposable labware under aseptic conditions.

4.8 Transfection of Murine 4T1 Cells

Murine 4T1 cells were seeded in 6-well plates [0.5×10^6 cells/well] in RPMI-1640 Media [3 mL] and incubated 14 to 16 h before transfection. On the day of transfection, a concentrated Stock Solution of Chol-RNAi Polyplexes [2 μ M Chol-RNAi] was prepared as described (Section 4.5) then diluted to 200 nM Chol-RNAi in Complete RPMI-1640 lacking FBS and antibiotics. Old growth media was aspirated and Complete RPMI-1640 lacking FBS and antibiotics alone or with diluted polyplexes [1.5 mL] were added for 4 h, then an equal volume of 20% FBS Complete RPMI-1640 [1.5 mL] was added before further incubation for 20 h (24 h from the start of transfection). Average murine STAT3 mRNA copy numbers per ng total RNA \pm propagated SD (n= 3 replicates from two independent treatments) were then determined by RT-ddPCR at the indicated time point (Section 4.9), normalized to untreated cells at the same time point, and compared at each time point by unpaired two-tailed t-test or vs. the 24 h time point by ordinary one-way ANOVA with Dunnett's post-test (GraphPad Prism 9.2.0).

4.9 Quantitation of murine STAT3 mRNA and Chol-RNAi by Reverse Transcription-Droplet Digital™ PCR (RT-ddPCR)

For mRNA, total purified RNA was quantitated by absorbance (NanoDrop 200), diluted in sterile, nuclease-free ddH₂O, and converted to cDNA [~ 1 μ g total] (Superscript™ VILO™ cDNA Synthesis Kit, Life Technologies). Murine STAT3 and murine HPRT mRNA copy numbers were then determined by droplet-digital PCR (ddPCR) (QX200 Droplet Digital PCR System, BioRad) from 10 ng of template cDNA using PrimeTime® Taqman assays (IDT, Coralville, USA) and BioRad ddPCR reagents / consumables.

For Chol-RNAi molecules, total purified RNA was diluted in sterile, nuclease-free deionized H₂O and converted to cDNA [~ 1 μ g total] (TaqMan™ MicroRNA Reverse Transcription Kit, Invitrogen™, ThermoFisher). Copy numbers of Chol-RNAi were quantitated by ddPCR using two different amounts of template cDNA [tumor: 6.67, 33.5 ng; lungs: 6.67, 33.35 ng (Chol-RNAi alone), 1.334, 13.4 ng (Chol-RNAi Polyplexes); liver: 1.334, 13.34 ng (Chol-RNAi alone), 0.1334, 1.334 (Chol-RNAi Polyplexes); spleen, kidneys: 0.2668, 1.334 ng; heart, brain: 13.34, 133.4 ng], using stem-loop quantitative Custom TaqMan Small RNA Assays (Invitrogen™, ThermoFisher) for the antisense strand of Chol-siSTAT3 or Chol-DsiSTAT3 and BioRad ddPCR reagents / consumables as directed.

Chol-RNAi antisense copies / μ L / ng template cDNA was calculated as the slope of Chol-RNAi antisense strand copies / μ L (y-axis) vs. mass of template cDNA (x-axis) (2 amounts). Mass of Chol-RNAi (ng) / mg tissue was then calculated by multiplying Chol-RNAi antisense copies / μ L / ng template cDNA with the slope from the standard curve of ng Chol-RNAi (y-axis) vs. Chol-RNAi antisense copies / μ L (x-axis) and dividing by the volume-normalized mass of the tissue sample [10 mg].

4.10 Potencies and kinetics of STAT3 mRNA suppression in primary murine 4T1 breast tumors by Chol-RNAi Polyplexes after i.v. administration

All procedures were approved by the University of Nebraska Medical Center Institutional Animal Care and Use Committee. Primary murine 4T1 breast tumors were prepared in female BALB/c mice (4 to 6 weeks old) as described [4] but hair was first removed from the region above the tumor cell inoculation site (mammary fat pad #4) by shaving /

applying Nair cream (removed with warm water and gauze after 30 sec then rinsed with 70% ethanol) and injecting 10-fold fewer 4T1 cells [5×10^5 4T1 cells total] SQ to facilitate tumor volume measurements by 3D surface scanning (TumorImager, Bioticon).

To determine the potencies of STAT3 mRNA suppression, primary 4T1 tumors were grown to 30 to 50 mm³ (Day 0) then vehicle alone [0.1M HEPES, 0.15M NaCl, pH 7.4, filter-sterilized] or vehicle containing the indicated Chol-RNAi Polyplex was injected by tail vein [0.1 mL] at the indicated equimolar doses of Chol-siSTAT3 or Chol-DsiSTAT3 or a single maximum dose of inactive Chol-siCTRL or Chol-DsiCTRL. After 48 h, primary tumors were isolated, cut into ~0.5 cm thick pieces, suspended in RNAlater (Thermo Fisher Scientific), and stored at -80°C. Total RNA was later isolated from three pieces of each tumor (RNeasy Lipid Tissue Mini Kit / TissueLyser, Qiagen) and average ratios of murine STAT3 to murine HPRT mRNA copy numbers \pm propagated SD (n = 5 mice, 3 tumor pieces from each mouse) were determined by ddPCR (Section 4.9) and normalized to vehicle alone.

To determine the kinetics of STAT3 mRNA suppression, primary 4T1 tumors were grown to 30 to 50 mm³ (Day 0) then vehicle alone [0.1M HEPES, 0.15M NaCl, pH 7.4, filter-sterilized] or vehicle containing the indicated Chol-RNAi Polyplexes was injected into the tail vein [0.1 mL] at an equimolar amount of Chol-siSTAT3 [0.41 mg/kg] or Chol-DsiSTAT3 [0.5 mg/kg]. After the indicated time points, average ratios of murine STAT3 to murine HPRT1 mRNA copy numbers \pm propagated SD (n = 5 mice, 3 tumor pieces each) normalized to vehicle alone were determined as described in this section.

4.11 Tumor growth delay of primary murine 4T1 breast tumors

All procedures were approved by the University of Nebraska Medical Center Institutional Animal Care and Use Committee. Primary 4T1 tumors were prepared in female BALB/c mice (Section 4.10). Tumor volumes and body weights were measured every other day before treatment, then daily until 48 h after the last treatment. When tumor volumes reached 30 to 50 mm³ (Day 0), vehicle alone [0.1M HEPES, 0.15M NaCl, pH 7.4, filter-sterilized] or vehicle containing the indicated Chol-RNAi Polyplexes was injected into the tail-vein [0.1 mL] at equimolar amounts of Chol-RNAi [2.0 mg Chol-siSTAT3/kg or 2.5 mg Chol-DsiSTAT3/kg] on days 0, 2, 4, and 6. Average daily tumor volumes \pm SD (n=5 mice) were compared at each time point by Multiple t-tests. A rate-based T/C ratio and associated *P* value [12] were calculated as directed using the author-provided excel spreadsheet. On Day 8 (48 h after final dose), tumors were isolated, stored at -80°C, and Stat3 protein levels were determined by Western Blot (Section 4.12).

4.12 Quantitation of Stat3 protein in primary 4T1 tumors by Western Blot

Total protein was extracted from thawed tumors using Cell Extraction Buffer (Invitrogen) containing 1 mM PMSF, 1X protease inhibitor cocktail, and 1X EDTA (Thermo Scientific) and quantified using pierce BCA protein assay (Thermo Scientific) as directed. Protein lysates [40 μ g] were resolved by SDS-PAGE (Mini-PROTEAN TGX Precast Protein Gels, Bio-Rad) and transferred (Mini Trans-Blot® Cell, BioRad) to PVDF membranes as directed. PVDF membranes were incubated with rocking in Blocking Buffer [5% (w/v) non-fat dry milk in TBST Buffer] (r.t., 1 h), rinsed with TBST (r.t., 5 sec), incubated with primary antibodies (β -actin [sc-47778] and Stat3 [sc-8019], Santa Cruz Biotechnology) [1:200 in TBST] (4°C, overnight), rinsed 3X with TBST (r.t., 5 min.), and incubated with secondary antibody (horseradish peroxidase-conjugated mouse IgG κ binding protein; m-IgG κ BP-HRP [sc-516102], Santa Cruz Biotechnology) [1:5000 in TBST (r.t., 1 h), and rinsed 3X with TBST as above. The blot was incubated with HRP substrate (Luminata Classico Western HRP, Sigma) as directed, visualized (MyECL imager, Thermo Scientific). Average ratios of Stat3 / β -Actin protein band intensities \pm SD (n=2 measurements) were then determined by imaging densitometry (ImageJ software) and compared by XXX.

4.13 Pharmacokinetics of Chol-RNAi after i.v. administration

All procedures were approved by the University of Nebraska Medical Center Institutional Animal Care and Use Committee. Chol-RNAi alone and Chol-RNAi Polyplexes were prepared for *in vivo* studies (Section 4.5) and injected [0.1 mL] into the tail veins of female BALB/c mice (n=5 mice) at equimolar doses [2.0 mg Chol-siSTAT3/kg or 2.5 mg Chol-DsiSTAT3/kg] (Section 4.10). Blood [~0.1 mL] from treated and untreated mice (plasma background) was collected into Li-heparinized tubes (0.3 mL Microvette Tubes, Sarstedt) from a submandibular bleed (5 mm Goldenrod lancet, Braintree Scientific) and plasma supernatants (2500 RCF, 15 min) [~50 μ L] were stored at -80°C . A standard curve was prepared by spiking Chol-siSTAT3, Chol-DsiSTAT3, Chol-siSTAT3 Polyplexes, or Chol-DsiSTAT3 Polyplexes [450, 225, 112.5, 56.3, 28.1, and 14.1 ng Chol-RNAi] into untreated plasma [5 μ L] (n=2 per standard).

Total RNA was isolated from plasma (miRNeasy Mini, Qiagen) with modifications by adding QIAzol Lysis Reagent at 3:1 plasma (v:v), vortexing, incubating (r.t., 5 min.), adding water-soluble cholesterol (Cholesterol-Water Soluble, Sigma) [1 mg/mL in deionized H₂O] at 1:2 plasma (v/v) then SDS [10%] at 3:1 plasma (v/v), heating (95 $^{\circ}\text{C}$, 5 min.) and cooling (2 min.) (4 cycles heating/cooling), adding chloroform at 10:1 plasma (v/v), vortexing, incubating (r.t., 2 min.), pelleting (13,000 RCF, 15 min., 2 times), adding 100% EtOH at 5:1 supernatant (v/v), and column purification as described (MiRNeasy Mini, Qiagen) then quantitated by ABS₂₆₀ (NanoDrop spectrophotometer, ThermoFisher Scientific).

Total RNA isolated from plasma [2 μ L] and Kit Diluent [98 μ L] (n=3 wells) were pipetted into a 96-well black (clear bottom) plate. Fluorophore (Quant-iTTM RiboGreen[®] RNA Reagent and Kit, Invitrogen) [1/1000 Dilution in Kit Diluent] [100 μ L] was added to each well, the plate was incubated (r.t., 2-5 min), and fluorescence (EX₄₈₀/EM₅₂₀) was measured (Molecular Devices SpectraMax ID3, top read). Samples and standards were diluted as necessary to fall within the linear range of fluorescence measurements. The average plasma concentration of Chol-siSTAT3 or Chol-DsiSTAT3 at each time point \pm propagated SD (n=5 mice) was then calculated as the difference between plasma concentrations of total RNA in treated vs. untreated plasma. Pharmacokinetic parameters were determined by non-compartmental analysis (Phoenix WinNonlin version 8.2, Certara, Princeton, NJ, USA). Area under the curve (AUC) was calculated using the linear log trapezoidal rule.

4.14 Distribution of Chol-RNAi molecules in tumors and organs after *i.v.* administration

All procedures were approved by the University of Nebraska Medical Center Institutional Animal Care and Use Committee. Chol-siSTAT3, Chol-DsiSTAT3, Chol-siSTAT3 Polyplexes, and Chol-DsiSTAT3 Polyplexes were prepared for *in vivo* studies (Section 4.5) and injected [0.1 mL] into the tail veins of female BALB/c mice (n=5 mice) at equimolar amounts [2.0 mg Chol-siRNA/kg or 2.5 Chol-DsiSTAT3/kg] (Section 4.10). After 15 min, mice were euthanized (isoflurane drop jar/cervical dislocation), blood was removed / organs were perfused (sterile PBS) by cardiac puncture, organs and tumors were isolated, weighed, suspended in RNAprotect Tissue Reagent (Qiagen) as directed, and stored at -80°C .

To isolate total RNA, two pieces of organ [lungs ~30 mg; liver ~50 mg; spleen ~30 mg; kidneys ~40 mg; heart ~15 mg; brain ~30 mg] or tumor [~10 mg] were thawed and initially homogenized (Precellys Evolution technology, Bertin Instruments) in QIAzol Lysis Reagent (Qiagen) [10 μ L QIAzol Lysis Reagent:1 mg tissue] on "Hard" mode. A standard curve for Chol-DsiSTAT3 and Chol-DsiSTAT3 Polyplexes was prepared for each organ or tumor by spiking in Chol-DsiSTAT3 or Chol-DsiSTAT3 Polyplexes [tumor, lungs, liver, spleen, kidneys: 0.6, 3, 15, 75, 150, 300 ng Chol-DsiSTAT3; heart, brain: 0.15, 0.3, 0.6, 3, 15, 75 ng Chol-DsiSTAT3] into the initial "Hard" mode homogenates of the respective organs or tumors isolated from untreated mice. SDS [5% (w/v) in deionized H₂O] [20 μ L:1 mg tissue] and water-soluble cholesterol (Sigma) [10 mg/mL in deionized H₂O] [0.2 μ L:1 mg tissue] was added to the initial "Hard" mode homogenates and further homogenized on "Soft" mode. A portion of the final homogenate [300 μ L; normalizes to 10 mg of tissue sample for RNA extraction] was heated (92 $^{\circ}\text{C}$, 5 min), cooled (r.t., 10 sec), and vortexed (4

cycles of heating, cooling, vortexing) [13]. Total RNA was extracted by column purification after preparing the final homogenate as directed (miRNeasy Mini Kit, Qiagen, Hilden, Germany) and quantitated by ABS₂₆₀ (NanoDrop spectrophotometer, ThermoFisher Scientific). The average mass Chol-DsiSTAT3 (ng) / mass of tissue (mg) \pm propagated SD (n=2 tissue/tumor pieces from n=5 mice) was quantitated by RT-ddPCR (Section 4.9) and compared in each tissue by nonparametric two-tailed t-tests with Holm-Sidak correction (GraphPad Prism 9.2.0).

5. Conclusions

In summary, we found that Chol-siRNA Polyplexes and Chol-DsiRNA Polyplexes formed with PLL[30]-PEG[5K] increase potency and efficacy against STAT3 mRNA to the same extent in primary murine syngeneic breast tumors although Chol-DsiRNA Polyplexes likely increase the duration of mRNA suppression as the frequency of tumor-saturating doses is increased. Thus, both Chol-siRNA Polyplexes and Chol-DsiRNA Polyplexes may be good clinical candidates to improve the RNAi therapy of breast cancer and other solid tumors.

Supplementary Materials: The following are available online at www.mdpi.com/xxx/s1, Figure S1: Representative Distributions of Chol-siCTRL Polyplex and Chol-DsiCTRL Polyplex Diameters, Figure S2: Effect of Inactive Chol-siCTRL Polyplexes and Chol-DsiCTRL Polyplexes on the growth of primary syngeneic murine 4T1 breast tumors after repeated i.v. treatments.

Author Contributions: Funding acquisition, J.A.V., D.W.C.; Project administration, J.A.V., Supervision, J.A.V., S.M.C., S.R.D., Y.A.; Conceptualization, J.A.V., R.K.S., D.W.C.; Resources, J.A.V., D.W.C.; Methodology, J.A.V., Z.Y., S.M.C., S.R.D., L.L.A.; Validation, J.A.V., S.M.C.; Investigation, Z.Y., M.M.A., S.M.C., L.L.A.; Formal analysis, J.A.V., Z.Y., M.M.A., S.M.C., S.R.D., L.L.A., D.K.; Data Curation, J.A.V., Z.Y., M.M.A., L.L.A.; Visualization, J.A.V.; Writing – original draft, J.A.V.; Writing – reviewing & editing, J.A.V., R.K.S., D.W.C., S.M.C., Y.A. All authors have read and agreed to the published version of the manuscript.

Funding: This work was supported by NIH/NCATS 1R41TR001902-01A1 (JAV), NIH/NCI R01CA228524 (RKS), Fred & Pamela Buffett Cancer Center Support Grant (P30CA036727), and Pediatric Cancer Research Group Support, State of Nebraska, LB 417 (DC, ZY).

Institutional Review Board Statement: The study was conducted according to the guidelines of the Declaration of Helsinki and approved by the Institutional Animal Care and Use Committee (IACUC) at the University of Nebraska Medical Center (protocol code 18-010-03-FC, 11 June 2019).

Acknowledgments: We thank the Comparative Medicine Research Technical Service at the University of Nebraska Medical Center for performing SQ and tail vein injections.

Conflicts of Interest: JAV is cofounder of a company that licenses the described technology.

References

1. Caillaud, M.; El Madani, M.; Massaad-Massade, L. Small interfering RNA from the lab discovery to patients' recovery. *Journal of controlled release : official journal of the Controlled Release Society* **2020**, *321*, 616-628, doi:10.1016/j.jconrel.2020.02.032.
2. Ye, Z.; Abdelmoaty, M.M.; Ambardekar, V.V.; Curran, S.M.; Dyavar, S.R.; Arnold, L.L.; Cohen, S.M.; Kumar, D.; Alnouti, Y.; Coulter, D.W.; et al. Preliminary preclinical study of Chol-DsiRNA polyplexes formed with PLL[30]-PEG[5K] for the RNAi-based therapy of breast cancer. *Nanomedicine* **2021**, *33*, 102363, doi:10.1016/j.nano.2021.102363.
3. Hager, S.; Fittler, F.J.; Wagner, E.; Bros, M. Nucleic Acid-Based Approaches for Tumor Therapy. *Cells* **2020**, *9*, doi:10.3390/cells9092061.
4. Ambardekar, V.V.; Wakaskar, R.R.; Sharma, B.; Bowman, J.; Vayaboury, W.; Singh, R.K.; Vetro, J.A. The efficacy of nuclease-resistant Chol-siRNA in primary breast tumors following complexation with PLL-PEG(5K). *Biomaterials* **2013**, *34*, 4839-4848, doi:10.1016/j.biomaterials.2013.03.021.
5. Grijalvo, S.; Alagia, A.; Jorge, A.F.; Eritja, R. Covalent Strategies for Targeting Messenger and Non-Coding RNAs: An Updated Review on siRNA, miRNA and anti-miR Conjugates. *Genes (Basel)* **2018**, *9*, doi:10.3390/genes9020074.

6. Chen, X.; Mangala, L.S.; Rodriguez-Aguayo, C.; Kong, X.; Lopez-Berestein, G.; Sood, A.K. RNA interference-based therapy and its delivery systems. *Cancer Metastasis Rev* **2018**, *37*, 107-124, doi:10.1007/s10555-017-9717-6.
7. Gao, S.; Dagnaes-Hansen, F.; Nielsen, E.J.; Wengel, J.; Besenbacher, F.; Howard, K.A.; Kjems, J. The effect of chemical modification and nanoparticle formulation on stability and biodistribution of siRNA in mice. *Mol Ther* **2009**, *17*, 1225-1233, doi:10.1038/mt.2009.91.
8. Ambardekar, V.V.; Wakaskar, R.R.; Ye, Z.; Curran, S.M.; McGuire, T.R.; Coulter, D.W.; Singh, R.K.; Vetro, J.A. Complexation of Chol-DsiRNA in place of Chol-siRNA greatly increases the duration of mRNA suppression by polyplexes of PLL(30)-PEG(5K) in primary murine syngeneic breast tumors after i.v. administration. *International Journal of Pharmaceutics* **2018**, *543*, 130-138, doi:10.1016/j.ijpharm.2018.03.045.
9. Ling, X.; Arlinghaus, R.B. Knockdown of STAT3 expression by RNA interference inhibits the induction of breast tumors in immunocompetent mice. *Cancer research* **2005**, *65*, 2532-2536, doi:10.1158/0008-5472.CAN-04-2425.
10. Huynh, J.; Chand, A.; Gough, D.; Ernst, M. Therapeutically exploiting STAT3 activity in cancer - using tissue repair as a road map. *Nature reviews. Cancer* **2018**, doi:10.1038/s41568-018-0090-8.
11. Dai, L.; Cheng, L.; Zhang, X.; Jiang, Q.; Zhang, S.; Wang, S.; Li, Y.; Chen, X.; Du, T.; Yang, Y.; et al. Plasmid-based STAT3-siRNA efficiently inhibits breast tumor growth and metastasis in mice. *Neoplasia* **2011**, *58*, 538-547.
12. Hather, G.; Liu, R.; Bandi, S.; Mettetal, J.; Manfredi, M.; Shyu, W.C.; Donelan, J.; Chakravarty, A. Growth rate analysis and efficient experimental design for tumor xenograft studies. *Cancer Inform* **2014**, *13*, 65-72, doi:10.4137/CIN.S13974.
13. Landesman, Y.; Svrzikapa, N.; Cognetta, A., 3rd; Zhang, X.; Bettencourt, B.R.; Kuchimanchi, S.; Dufault, K.; Shaikh, S.; Gioia, M.; Akinc, A.; et al. In vivo quantification of formulated and chemically modified small interfering RNA by heating-in-Triton quantitative reverse transcription polymerase chain reaction (HIT qRT-PCR). *Silence* **2010**, *1*, 16, doi:10.1186/1758-907X-1-16.